RSC Advances

PAPER

View Article Online
View Journal | View Issue

Cite this: *RSC Adv.*, 2016, **6**, 25179

An organic terpyridyl-iron polymer based memristor for synaptic plasticity and learning behavior simulation†

Xi Yang,‡[acd] Cheng Wang,‡[b] Jie Shang,‡[cd] Chaochao Zhang,[cd] Hongwei Tan,[cd] Xiaohui Yi,[cd] Liang Pan,[cd] Wenbin Zhang,[cd] Fei Fan,[bd] Yaqing Liu,*[a] Yu Chen,*[b] Gang Liu*[cd] and Run-Wei Li[cd]

Received 1st February 2016
Accepted 1st March 2016

DOI: 10.1039/c6ra02915a

www.rsc.org/advances

Memristors have been extensively studied for nonvolatile memory storage, neuromorphic computing, and logic applications. Particularly, synapse emulation is viewed as a key step to realizing neuromorphic computing, because the biological synapse is the basic unit for learning and memory. In this study, a memristor with the simple structure of Ta/viologen diperchlorate [EV(ClO_4)$_2$]/terpyridyl-iron polymer (TPy-Fe)/ITO is fabricated to simulate the functions of the synapse. Essential synaptic plasticity and learning behaviours are emulated by using this memristor, such as spike-timing-dependent plasticity and spike-rate-dependent plasticity. It is demonstrated that the redox between a terpyridyl-iron polymer and viologen species leads to our memristor behavior. Furthermore, the learning behavior depending on different amplitudes of voltage pulses is investigated as well. These demonstrations help pave the way for building bioinspired neuromorphic systems based on memristors.

Introduction

With the increasing demand of information storage and processing, the classical von Neumann system of digital computers suffers more and more from the inefficiency of serial mode operation, as well as the higher power consumption problems.[1–3] Among various solutions to break the von Neumann bottleneck, imitating neural networks in human brains is considered to be the effective method.[4–6] Neuromorphic computing is a bio-inspired approach that could be more efficient due to its parallel processing capability.[7–9] In human brains, neuron is the basic structure and functioning unit of the nervous system. While, the synapses are the significant parts between neurons, which perform the processing and transmission of the information.[10–13] Therefore, synapse is generally considered as the smallest unit of memory and learning in human brain. The synaptic weight between two neurons can be accurately modulated by the ionic flow. It is widely reviewed that the learning behaviour and functions of the biological synaptic systems can be emulated by adapting the synaptic weights.[14–16] Thus, emulating the functions of the biological synapses is vital to realizing neuromorphic computing. The memristor (memory + resistor), an electrical device, has nonlinear transmission characteristics that are similar to certain properties of biological synapse. Resembling a biological synapse, the conductance of the memristor can be gradually regulated by controlling charge fluxes.[17–21] These characteristics of the memristor can be used to simulate the synaptic behaviors, desired to achieve the construction of artificial network.[22]

So far, abundant amount of efforts have been devoted to exploiting biomimicking memristors, most of which are concentrated on inorganic materials and devices that need elaborated fabrication procedures.[23–29] On the contrary, organic systems that make the use of charge transfer and electrochemical redox effects to change the device resistance usually demonstrate the advantages of low cost, easy fabrication, mechanical flexibility and especially, tunable electronic properties by designing molecular structure.[30–35] In this study, we report the memristive behavior in the ethyl viologen diperchlorate [EV(ClO_4)$_2$]/terpyridyl-iron polymer (TPy-Fe) organic redox system. The polymer TPy-Fe with coordinating bond between Fe cation and pyridine ring is used in this study for its electrochemical redox behavior,[36] while ethyl viologen diperchlorate [EV(ClO_4)$_2$] is used as counter reaction material for TPy-Fe oxidation which also provides transportable perchlorate

[a]*School of Materials Science and Engineering, North University of China, Taiyuan, Shanxi 030051, China. E-mail: zfflyq98@163.com*

[b]*Institute of Applied Chemistry, East China University of Science and Technology, Shanghai 200237, China. E-mail: chentangyu@yahoo.com*

[c]*Key Laboratory of Magnetic Materials and Devices, Ningbo Institute of Materials Technology and Engineering, Chinese Academy of Sciences, Ningbo, 315201, P. R. China. E-mail: liug@nimte.ac.cn; Fax: +86-574-8668-5163; Tel: +86-574-8668-5030*

[d]*Zhejiang Province Key Laboratory of Magnetic Materials and Application Technology, Ningbo Institute of Materials Technology and Engineering, Chinese Academy of Sciences, Ningbo, 315201, P. R. China*

† Electronic supplementary information (ESI) available. See DOI: 10.1039/c6ra02915a

‡ These authors contribute equally to this work.

ions to neutralize the charged form of the polymer.[37,38] To improve the migration rate of the perchlorate ion, polyethylene oxide (PEO) acts as a solid electrolyte in $EV(ClO_4)_2$ layer.[39] The electrical properties of the organic redox system is evaluated in a two-terminal devices with sandwich structure of Ta/$EV(ClO_4)_2$ + PEO/TPy-Fe/ITO, presenting memrisitive behaviour that can be used to emulate the potentiation and depression processes of a biological synapse. Consequently, a series of synaptic behaviors, including the spike-rate-dependent plasticity (SRDP), the spike-timing-dependent-plasticity (STDP), short-term memory (STM) and long-term memory (LTM), and learning behaviors, are successfully mimicked, demonstrating the feasibility of using organic materials to construct synaptic mimicking memristor devices.

Results and discussion

The chemical structure of the coordination polymer TPy-Fe, with the bis-terpyridine ligands connected to the transition metal ions of Fe,[40,41] is verified through ^{1}H nuclear magnetic resonance (^{1}H NMR) and X-ray photoelectron spectroscopy (XPS) and shown in Fig. 1a. The ^{1}H NMR spectrum (Fig. 1b) reveals proton signals of the pyridines rings with chemical shifts of 10.40–9.58 (m, 4H), 9.54–7.78 (m, 12H), as well as that of the benzene rings at ~7.10–7.74 (m, 8H) for the coordination polymer TPy-Fe. The XPS spectrum of Fe 2p for TPy-Fe is shown in Fig. 1c. The binding energies of the Fe $2p_{3/2}$ and Fe $2p_{1/2}$ peaks are 708.7 eV and 721.5 eV, respectively. An obvious satellite signal, which does not overlap with either the Fe $2p_{3/2}$ or Fe $2p_{1/2}$ peaks, is located at 714.3 eV. The binding energy difference between the Fe $2p_{3/2}$ peak and the satellite peak was approximately 6 eV. The presence of this 'shoulder' satellite peak and the binding energy difference of 6 eV are consistent with the that reported in the literatures,[42–46] and are clear evidence of the existence of Fe^{2+} ions. As such, it can be confirmed that the coordination polymer TPy-Fe with bivalent iron species has been prepared successfully. The chemical structure of $EV(ClO_4)_2$ and PEO are also shown in Fig. 1a.

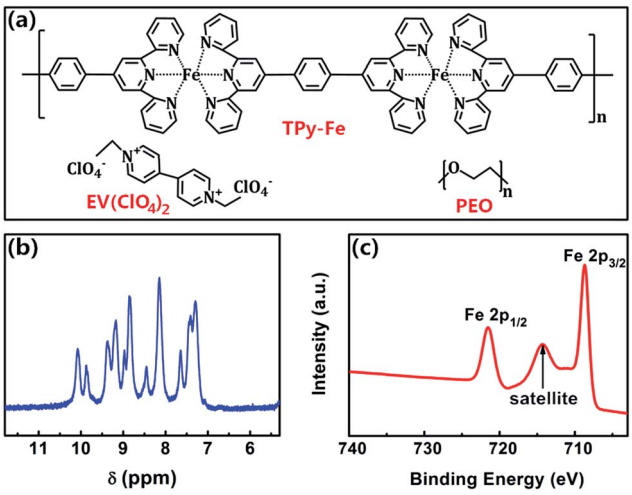

Fig. 1 (a) Chemical structures of TPy-Fe, $EV(ClO_4)_2$ and PEO. (b) ^{1}H nuclear magnetic resonance (^{1}H NMR) spectrum of polymer TPy-Fe. (c) X-ray photoelectron spectrum (XPS) of the TPy-Fe polymer film.

The fundamental memristive behaviors of the Ta/$EV(ClO_4)_2$ + PEO/TPy-Fe/ITO device are shown in the current–voltage (I–V) characteristics of Fig. 2a. To measure these behaviors, the device is subjected to eight consecutive positive voltage sweeps of 0 V → 3 V → 0 V. Initially, the Ta/$EV(ClO_4)_2$ + PEO/TPy-Fe/ITO memristor shows a high resistance of $\sim 2.9 \times 10^{10}$ Ω (read at 0.1 V). Then, the current value increases gradually, and the device resistance decreases gradually to 1.8×10^9 Ω. When the voltage sweepings are reversed to 0 V → −2 V → 0 V, the current value decreases continuously with the number of sweepings, while the device resistance increases constantly from 3.8×10^8 Ω to 2.5×10^9 Ω (read at −0.1 V). When positive electric field is applied, Fe(II) ions are oxidized to Fe(III) ions, while EV(II) species are reduced to EV(I).[37–39] During this process, the band gap of the polymer can be changed with the oxidation and introduction of impurity energy levels. In the negative scans, reverse redox reactions occur (see ESI, Fig. S2 and S3†). Consequently, the conductance of the device can be adjusted continuously by voltage stimulation, which is similar to the non-linear transmission characteristics of biological synapses.[26] The conductivity or the current value can be regarded as synaptic weights. A rectifying effect is also observed during the sweeping process, which may be ascribed to the difference in the molecular orbital energy levels between the TPy-Fe polymer and the $EV(ClO_4)_2$. Such a rectifying effect is useful for the single-direction transmission of information in biological synapses. Many biological synapses in the brain are rectifying in that they allow information transmission along a single direction.[47,48]

The potentiation and depression of the synaptic weight are another fundamental synaptic behavior that the excitability of synapses can be incrementally adjusted through the action potential spikes.[49] In our study, the potentiation and depression of the synaptic weight can be considered as the increase and decrease of the device current as mentioned above, which are obtained by applying a series of 50 positive pulses (3 V, 10 ms) immediately followed by 50 negative pulses (−2 V, 10 ms) as shown in Fig. 2b. The current value was read by a small read

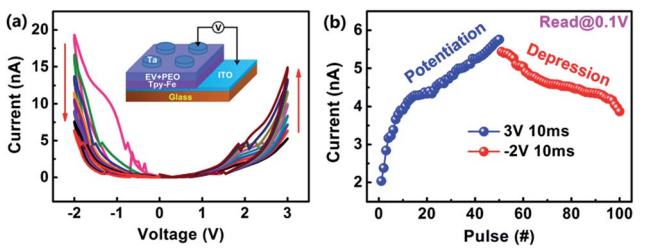

Fig. 2 (a) Current–voltage characteristics of the Ta/$EV(ClO_4)_2$ + PEO/TPy-Fe/ITO memristor showing non-linear transmission behavior similar to that of a biological synapse. The inset is the schematic illustration of our memristor. (b) Device current in response to a series of positive and negative voltage stimulations showing the respective potentiation and depression of the synaptic weight. The amplitude, duration and period of the positive voltage pulse and the negative voltage pulse are +3 V, 10 ms, 2 s and −2 V, 10 ms, 2 s, respectively. The current responses are read with a small voltage of ±0.1 V.

voltage of ±0.1 V after each pulse. The synaptic weight of our memristor can be strengthened or weakened with the positive or negative pulses, respectively. It is noteworthy that a gap between the final state of potentiation and the initial state of depression is observed. This can be understood by the spontaneous back drift of the perchlorate ions with the absence of electrical driving forces.

The device conductivity can also be modulated by tuning the duration and amplitude of the applied voltage pulses, which emulate the spike-rate-dependent plasticity (SRDP) of biological synapses.[50,51] SRDP is one basic characteristics of biological synaptic plasticity, which is obtained by BCM model proposed by Bienenstock, Cooper, and Munro.[52] It declares that the pre-synaptic spiking rate greatly influences the synaptic weight. In the present study we have applied voltage pulse stimulations with a fixed number of 10 and different frequencies from 1 Hz to 20 Hz on the memristor devices, as shown in Fig. 3a. The change of firing frequencies from 1 Hz to 20 Hz is the same as the change of the pulse-to-pulse intervals from 1 s to 0.05 s. It is found that the current value clearly increases with frequency increasing. For the sake of quantitatively studying the transformation of the current recorded at every frequency, we calculated the relative changes in synaptic weight and plotted it *versus* stimulation frequency, as shown in Fig. 3b. At the frequency of 1 Hz, there is little enhancement of the device current with the increasing stimulation numbers. When the frequency reaches to 20 Hz, the device current increases for more than 20 times. More frequent stimulation leads to a larger change of the synaptic weight.

Spiking-timing-dependent plasticity (STDP) is the synaptic plasticity that follows the Hebbian learning rule.[53] STDP suggests that the synaptic weight can be regulated by the time interval between pre- and post-synaptic spikes. We define the TE (Ta) and BE (ITO) of the memristor as a pre-synaptic membrane and a post-synaptic membrane, respectively. Meanwhile, a pair of voltage pulses, which consists of a positive pulse with the amplitude of +3 V, duration of 10 ms and a negative pulse with the amplitude of 2 V, duration of 10 ms, has been imposed onto the device. A 2 s interval presents between the positive pulse and negative pulse. In Fig. 3c, Δt is defined as the interval between pre- and post-synaptic spikes ($\Delta t = t_{pre} - t_{post}$). The change of the synaptic weight (ΔW) is considered as $(I_2 - I_1)/I_1$, where I_1 and I_2 denote the currents obtained before and 10 min after the pulse-pairs removed, respectively. If the post-synapse stimulation momentarily arrives before the pre-synapse stimulation, which means $\Delta t < 0$, the synaptic weight gets increased; whereas if the pre-synapse stimulation arrives earlier than the post-synapse stimulate, which means $\Delta t > 0$, the synaptic weight becomes decreased. Furthermore, both the depression and potentiation of the synaptic weights show negative correlation to the interval between the pulse-pairs. The longer time interval Δt, the smaller the absolute value of ΔW. These results are shown in Fig. 3d. Therefore, by means of accurately controlling the interval and order between the pulse-pairs, we can successfully emulate the STDP of the biological synapse.

Generally, there are two fundamental characteristics that can describe the memory behavior in human brains: short-term memory (STM) and long-term memory (LTM). STM is the transient phenomenon, which only lasts for a few seconds or minutes and then fades away to its initial value.[54,55] On the other hand, LTM shows a permanent change in synaptic structures, which could persist for hours or days, even to years.[56] Besides, STM can be transformed to LTM through repeated rehearsals.[57,58] Both behaviors are observed in our memristor devices, as shown in Fig. 4a. We first apply 10 voltage pulses with fixed amplitude, widths and period to the $EV(ClO_4)_2$ + PEO/TPy-Fe memristor, then remove the stimulating voltage pulses and track the current value at reading voltage pulse (0.1 V, 10 ms). It is observed that the synaptic weight of the memristor falls off rapidly at the beginning, then arrives a stable value with time. This equals the STM behavior. In order to quantitatively calculate the STM behavior of the memristor, we use the modified Kohlrausch equation to describe the relaxation process as following,[59–61]

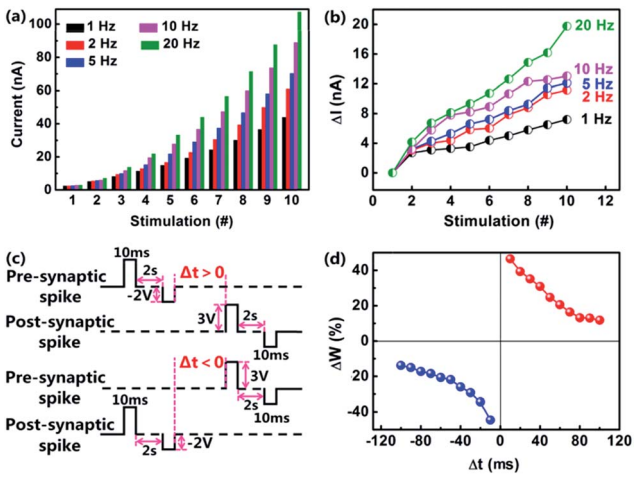

Fig. 3 Frequency-dependent synaptic potentiation and spike-rate-dependent plasticity (SRDP) of the $EV(ClO_4)_2$ + PEO/TPy-Fe memristor. Evolution of the device (a) current and (b) current change (ΔI) with 10 voltage pulse stimulations at different frequencies. Spike-timing-dependent plasticity (STDP) of the $EV(ClO_4)_2$ + PEO/TPy-Fe memristor. (c) The profiles of the pre-synaptic and post-synaptic spikes consisting of a voltage pulse pair with the amplitude, duration and separation of 3 V, 10 ms, 2 s and −2 V, 10 ms, 2 s respectively. (d) Change of the synaptic weight with the relative timing Δt of the pre-synaptic and post-presynaptic spike-pair application.

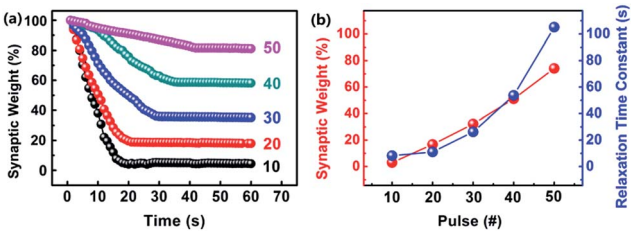

Fig. 4 Memory enhancement of the $EV(ClO_4)_2$ + PEO/TPy-Fe memristor. (a) Experimental (symbols) and fitted (solid lines) memory retention performance after being subjected to different numbers of identical voltage pulse stimulations. (b) Evolution of the relaxation time constant (τ) and the stabilized synaptic weight (I_0) along with the stimulating numbers.

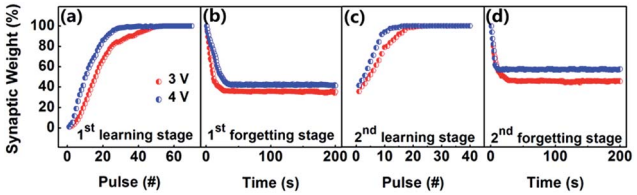

Fig. 5 The learning and forgetting behavior of the $EV(ClO_4)_2$ + PEO/TPy-Fe memristor under voltage stimulation pulses of different amplitudes in the (a) 1st learning, (b) 1st forgetting, (c) relearning and (d) 2nd forgetting processes, respectively.

$$I(t) = I_0 + A\exp(-t/\tau) \quad (1)$$

where $I(t)$ and I_0 are the synaptic weights at the time of t and that in the stable state, respectively, A is the pre-exponential factor and τ is relaxation time constant. When the relaxation time constant $\tau > t$, the synaptic weight drops fast. On the contrary, if $\tau \ll t$, the synaptic weight changes slowly. It is found that as the number of the stimulating pulses increases, both the relaxation time constant and stable synaptic weight increases significantly (Fig. 4b). For instance, the synaptic connection fades away in about 20 s when stimulated by 10 times. With the number of voltage pulses increased to 50, the speed of memory loss decreases and the remaining memory increases. This equals to transition from STM to LTM.

Fig. 5a–d shows another vital memory behavior in our device, which is called as learning behavior. At first, 50 consecutive voltage pulses are applied on our memristor, and the synaptic weight gradually increases with the number of stimulation pulses (Fig. 5a). We defined the growing process as "learning". When the applied voltage is removed, the synaptic weight decays to a mid-state without any external inputs (Fig. 5b). We defined the decaying process as "forgetting". However, only 20 subsequent stimulations can recover the synaptic weight to the original level of the first learning (Fig. 5c), which is defined as the "relearning" (or recalling) behavior. The synaptic weight also decreases to a stable state after removing the recalling stimulations, with a decay rate much slower than the first process of decaying (Fig. 5d). So, the process of learning, forgetting and relearning composes the learning behavior of the memristor, which demonstrates that the learned information will be more easily recalled.[24,26,62] Moreover, it can be seen that as the amplitude of the stimulation voltage pulses increased from 3 V to 4 V, the learning and relearning processes can be run much faster and more effective in the present memristive synapse, while the forgetting process get effectively weakened. This is similar to the fact that important events can results in strong memory in the brain of human beings.

Experimental

Materials

All chemicals were reagent grade and used without purification. Ethylene glycol (EG) and methanol (MeOH) were used as reaction solvents, which were purchased from Aldrich (Shanghai, China) and utilized without further purification. 4′,4‴-(1,4-Phenylene)bis(2,2′:6′,2″-terpyridine) (97%) and iron(II) acetate [$Fe(OAc)_2$, >99.99%] were purchased from Aldrich and used without further purification. The supporting electrolytes, lithium perchlorate ($LiClO_4$, 99%), tetrabutylammonium perchlorate (TBAP, 98%), and silver nitrate ($AgNO_3$, 99%) were purchased from Aldrich and used without further purification.

Instruments

The ^{1}H nuclear magnetic resonance (^{1}H NMR) spectra were performed at 400 MHz on a Bruker 400 AVANCE III spectrometer with dimethyl sulfoxide (DMSO) as solvent and tetramethylsilane (TMS) as a reference for the chemical shifts. The UV-visible absorption spectra of the polymer were obtained in diluted solution on a Shimadzu UV-2450 UV-Visible spectrophotometer. Steady-state fluorescence spectra of the polymer devices were recorded on an Andor SR303i-A/DU420A-BVF spectrofluorometer. Cyclic voltammetry (CV) measurements were measured in an electrolyte solution of TBAP in acetonitrile (0.1 M) under an argon atmosphere, using platinum gauze and Ag/AgCl as the counter and reference electrodes respectively. A typical scan rate of 20 mV s^{-1} was used during the CV measurements. Viscosity average molecular weight (M_v) was calculated by measured viscosity. The viscosity of Tpy-Fe polymer was tested by Ubbelohde viscometer.

Synthesis of monomer and polymer

The TPy-Fe coordination polymer was synthesized *via* stepwise polymerization with 4′,4‴-(1,4-phenylene)bis(2,2′:6′,2″-terpyridine) (denoted as chemical L1 for short) and $Fe(OAc)_2$ (Scheme S1, ESI†).[41] In detail, a mixture of $Fe(OAc)_2$ (60 mg, 0.5 mmol) and L1 (45 mg, 0.5 mmol) was refluxed in argon-saturated $HOCH_2CH_2OH$ at 120 °C for 24 h. Afterwards, the reaction solution was cooled to room temperature and then filtered to remove insoluble residues with Buchner funnel. A 100 mL round bottom flask, equipped with a reflux condenser, was degassed (flamed under vacuum) and filled with argon. The obtained powders packed with paper were extracted with tetrahydrofuran (THF) during 5 h, refluxing in a Soxhlet apparatus. The evaporated substances were small molecules and impurities. The residues within the paper were the required products. The product was placed in Petridish and dried in vacuum oven at 60 °C for 24 h. ^{1}H NMR (400 MHz, $CDCl_3$, ppm): 10.40–9.58 (m, 4H), 9.54–7.78 (m, 12H), 7.10–7.74 (m, 8H). M_v (the viscosity-average molecular weight) = 8.82×10^4.

Device fabrication and characterization

The ITO/glass substrates (Hefei Ke Jing Materials technology Co., LTD.) were pre-cleaned in the ethanol and acetone in an ultrasonic bath, each for 30 min in that order. The TPy-Fe solution of 3 mg mL^{-1} was prepared by dissolving the powders in dimethyl formamide (DMF) through magnetic stirring. In order to remove any dissolved particles, the as-prepared solutions were filtrated by the polytetrafluoroethylene (PTFE) membrance micro-filters with a 0.45 μm pore size. Then the TPy-Fe solution was spin-coated onto the pre-cleaned ITO/glass

substrate at 300 rpm for 20 s and then at 2000 rpm for 60 s, followed by heating at 50 °C overnight. The electrolyte solution was prepared according to the reported method.[39] The Ta top electrodes of 100 nm thickness were deposited by magnetron sputtering using a metal shadow mask at room temperature. The electrical properties of the Ta/EV$(ClO_4)_2$ + PEO/TPy-Fe/ITO devices were measured with a Keithley 4200 semiconductor characterization system under sweeping or pulse mode under an ambient atmosphere.

Conclusions

To summarize, coordination polymer with iron ions have been successfully synthesized and demonstrate several primary synaptic functions in Ta/EV$(ClO_4)_2$ + PEO/TPy-Fe/ITO structured memristor devices. Based on the reversible redox behaviors of the terpyridyl-iron polymer and viologen species, nonlinear transmission characteristics, potentiation and depression of the synaptic weight, SRDP, STRP, STM/LTM, as well as the learning–forgetting–relearning behaviors have been simulated. The present work shows the possibility of using organic materials for constructing the neuromorphic information storage and processing systems.

Acknowledgements

This work was supported by the State Key Project of Fundamental Research of China (973 Program, 2012CB933004), National Natural Science Foundation of China (51303194, 61328402, 61306152, 11474295, 61574146, 51525103), the Instrument Developing Project of the Chinese Academy of Sciences (YZ201327), the Youth Innovation Promotion Association of the Chinese Academy of Sciences, Ningbo Science and Technology Innovation Team (2015B11001), Ningbo Major Project for Science and Technology (2014B11011), Ningbo Natural Science Foundations (2014A610152), and Ningbo International Cooperation Projects (2014D10005).

References

1 J. Von Neumann, *The computer and the brain*, Yale University Press, New Haven, 2nd edn, 2000, pp. 327–358.
2 G. Perea and A. Araque, *J. Neurosci.*, 2005, **25**, 2192–2196.
3 G. Perea, M. Nevarrete and A. Araque, *Trends Neurosci.*, 2009, **32**, 421–425.
4 G. Indiveri, E. Chicca and R. Douglas, *IEEE Trans. Neural Netw.*, 2006, **17**, 211–221.
5 C. Mead, *Proc. IEEE*, 1990, **78**, 1629–1636.
6 S. Fusi, M. Annunziato, D. Badoni, A. Salamon and D. Amit, *Neural Comput.*, 2000, **12**, 2227–2258.
7 B. Pakkenberg and H. J. G. Gundersen, *J. Comp. Neurol.*, 1997, **384**, 312–320.
8 R. Douglas, M. Mahowald and C. Mead, *Annu. Rev. Neurosci.*, 1995, **18**, 255–281.
9 R. Waser, *Nanotechnology: Information Technology II*, Wiley-VCH, Germany, 2008, vol. 4, pp. 251–285.
10 B. Pakkenberg, D. Pelvig, L. Marner, M. J. Bundgaard, H. J. G. Gundersen, J. R. Nyengaard and L. Regeur, *Exp. Gerontol.*, 2003, **38**, 95–99.
11 C. Diorio, P. Hasler, A. Minch and C. A. Mead, *IEEE Trans. Electron Devices*, 1996, **43**, 1972–1980.
12 P. Hafliger and M. Mahowald, *Analog Integr. Circuits Signal Process.*, 1999, **18**, 133–138.
13 S. Yu, Y. Wu, R. Jeyasingh, D. Kuzum and H.-S. Wong, *IEEE Trans. Electron Devices*, 2011, **58**, 2729–2737.
14 S. Kim, S. H. Choi and W. Lu, *ACS Nano*, 2014, **8**, 2369–2376.
15 G. Q. Bi and M. M. Poo, *J. Neurosci.*, 1998, **18**, 10464–10472.
16 G. Q. Bi and M. M. Poo, *Nature*, 1999, **401**, 792–796.
17 L. O. Chua, *IEEE Trans. Circuit Theory*, 1971, **18**, 507–519.
18 L. O. Chua and S. M. Kang, *Proc. IEEE*, 1976, **64**, 209–223.
19 D. B. Strukov, G. S. Snider, D. R. Stewart and R. S. Williams, *Nature*, 2008, **453**, 80–83.
20 T. Hasegawa, T. Ohno, K. Terabe, T. Tasuruoka, T. Nakayama, J. K. Gimzewski and M. Aono, *Adv. Mater.*, 2010, **22**, 1831–1834.
21 T. Hasegawa, A. Nayak, T. Ohno, K. Terabe, T. Tasuruoka, J. K. Gimzewski and M. Aono, *Appl. Phys. A*, 2011, **102**, 811–815.
22 H.-S. P. Wong and S. Salahuddin, *Nat. Nanotechnol.*, 2015, **10**, 191–194.
23 S. H. Jo, T. Chang, I. Ebong, B. B. Bhadviya, P. Mazumder and W. Lu, *Nano Lett.*, 2010, **10**, 1297–1301.
24 T. Ohno, T. Hasegawa, T. Tsuruoka, K. Terabe, J. K. Gimzewski and M. Aono, *Nat. Mater.*, 2011, **10**, 591–595.
25 Z. Q. Wang, H. Y. Xu, X. H. Li, H. Yu, Y. C. Liu and X. J. Zhu, *Adv. Funct. Mater.*, 2012, **22**, 2759–2764.
26 T. Chang, S. H. Jo and W. Lu, *ACS Nano*, 2011, **5**, 7669–7676.
27 P. Krzysteczko, J. Munchenberger, M. Schafers, G. Reiss and A. Thomas, *Adv. Mater.*, 2012, **24**, 762–766.
28 D. Kuzum, R. G. D. Jeyasingh, B. Lee and H. S. P. Wong, *Nano Lett.*, 2012, **12**, 2179–2186.
29 F. Pan, S. Gao, C. Chen, C. Song and F. Zeng, *Mater. Sci. Eng., R*, 2014, **83**, 1–59.
30 Y. Chen, G. Liu, C. Wang, W. Zhang, R.-W. Li and L. Wang, *Mater. Horiz.*, 2014, **1**, 463–556.
31 G. Liu, C. Wang, W. Zhang, L. Pan, C. Zhang, X. Yang, F. Fan, Y. Chen and R.-W. Li, *Adv. Funct. Mater.*, 2015, **24**, 1500298.
32 N. R. Hosseini and J.-S. Lee, *ACS Nano*, 2015, **9**, 419–426.
33 W.-P. Lin, S.-J. Liu, T. Gong, Q. Zhao and W. Huang, *Adv. Mater.*, 2014, **26**, 570–660.
34 G. Y. Wen, Z. J. Ren, D. M. Sun, T. J. Zhang, L. L. Liu and S. K. Yan, *Adv. Funct. Mater.*, 2014, **24**, 3446–3455.
35 D. M. Sun, Z. M. Yang, Z. J. Ren, H. H. Li, M. R. Bryce, D. G. Ma and S. K. Yan, *Chem.–Eur. J.*, 2014, **20**, 16233–16241.
36 C.-W. Hu, T. Sato, J. Zhang, S. Moriyama and M. Higuchi, *J. Mater. Chem. C*, 2013, **1**, 3408–3413.
37 B. Han, Z. Li, T. Wandlowski, A. Baszczyk and M. Mayor, *J. Phys. Chem. C*, 2007, **111**, 13855–13863.
38 B. Liu, A. Baszczyk, M. Mayor and T. Wandlowski, *ACS Nano*, 2011, **5**, 5662–5672.
39 R. Kumar, R. G. Pillai, N. Pekas, Y. Wu and R. L. McCreery, *J. Am. Chem. Soc.*, 2012, **134**, 14869–14876.

40 K. A. Aamer and G. N. Tew, *Macromolecules*, 2007, **40**, 2737–2744.
41 F. S. Han, M. Higuchi, T. Ikeda, Y. Negishi, T. Tsukuda and D. G. Kurth, *J. Mater. Chem.*, 2008, **18**, 4555–4560.
42 T. Yamashita and P. Hayes, *Appl. Surf. Sci.*, 2008, **254**, 2441–2449.
43 S. J. Roosendaal, B. van Asselen, J. W. Elsenaar, A. M. Vredenberg and F. H. P. M. Habraken, *Surf. Sci.*, 1999, **442**, 329–337.
44 P. C. J. Graat and M. A. J. Somers, *Appl. Surf. Sci.*, 1996, **100**, 36–40.
45 P. Mills and J. L. Sullivan, *J. Phys. D: Appl. Phys.*, 1983, **16**, 723–732.
46 M. Muhler, R. Schlögl and G. Ertl, *J. Catal.*, 1992, **138**, 413–444.
47 M. E. Bear, B. W. Connors and M. A. Paradiso, *Neuroscience: Exploring the Brain*, High Education Press, Beijing, 2007, pp. 761–793.
48 R. C. Atkinson and R. M. Shiffrin, *The psychology of learning and motivation: advances in research and theory*, Academic Press, New York, 1968, pp. 89–195.
49 P. D. Grimwood, S. J. Martin and R. G. M. Morris, *Synapse*, John Hopkins University Press, Baltimore, 2001, pp. 519–535.
50 S. Li, F. Zeng, C. Chen, H. Liu, G. Tang, S. Gao, C. Song, Y. Lin, F. Pan and D. Guo, *J. Mater. Chem. C*, 2013, **1**, 5292–5298.
51 H. Markram, A. Gupta, A. Uziel, Y. Wang and M. Tsodyks, *Neurobiol. Learn. Mem.*, 1998, **70**, 101–112.
52 L. N. Cooper and M. F. Bear, *Nat. Rev. Neurosci.*, 2012, **13**, 798–810.
53 P. Häfliger and M. Mahowald, *Analog Integr. Circuits Signal Process.*, 1999, **18**, 133–139.
54 J. A. Kauer and R. C. Malenka, *Nat. Rev. Neurosci.*, 2007, **8**, 844–858.
55 G. Daoudal and D. Debanne, *Learn. Mem.*, 2003, **10**, 456–465.
56 C. H. Bailey and E. R. Kandel, *Annu. Rev. Physiol.*, 1993, **55**, 397–426.
57 K. A. Paller and A. D. Wagner, *Trends Cognit. Sci.*, 2002, **6**, 93–102.
58 F. I. Craik and M. J. Watkins, *J. verb. Learn. verb. Behav.*, 1973, **12**, 599–607.
59 B. Sturman, E. Podivilov and M. Gorkunov, *Phys. Rev. Lett.*, 2003, **91**, 176602.
60 J. T. Wixted and E. B. Ebbesen, *Psychol. Sci.*, 1991, **2**, 409–415.
61 D. C. Rubin, S. Hintin and A. Wenzel, *J. Exp. Psychol.*, 1999, **25**, 1161–1176.
62 W. T. Greenough, J. E. Black and C. S. Wallace, *Child Dev.*, 1987, **58**, 539–559.